Received: 22 September 2022 | Revised: 29 November 2022 | Accepted: 3 December 2022

DOI: 10.1111/pce.14506

ORIGINAL ARTICLE

Plant, Cell & Environment | WILEY

Optimal coordination and reorganization of photosynthetic properties in C_4 grasses

Haoran Zhou[1,2] | Erol Akçay[3] | Brent Helliker[3]

[1]School of Earth System Science, Institute of Surface-Earth System Science, Tianjin University, Tianjin, China

[2]School of the Environment, Yale University, New Haven, Connecticut, USA

[3]Department of Biology, University of Pennsylvania, Philadelphia, Pennsylvania, USA

Correspondence

Haoran Zhou, School of Earth System Science, Institute of Surface-Earth System Science, Tianjin University, Tianjin 300072, China.
Email: zhouhaoran06@gmail.com

Funding information

UCAR's Cooperative Programs for the Advancement of Earth System Science; NSF-IOS

Abstract

Each of >20 independent evolutions of C_4 photosynthesis in grasses required reorganization of the Calvin–Benson-cycle (CB-cycle) within the leaf, along with coordination of C_4-cycle enzymes with the CB-cycle to maximize CO_2 assimilation. Considering the vast amount of time over which C_4 evolved, we hypothesized (i) trait divergences exist within and across lineages with both C_4 and closely related C_3 grasses, (ii) trends in traits after C_4 evolution yield the optimization of C_4 through time, and (iii) the presence/absence of trends in coordination between the CB-cycle and C_4-cycle provides information on the strength of selection. To address these hypotheses, we used a combination of optimality modelling, physiological measurements and phylogenetic-comparative-analysis. Photosynthesis was optimized after the evolution of C_4 causing diversification in maximal assimilation, electron transport, Rubisco carboxylation, phosphoenolpyruvate carboxylase and chlorophyll within C_4 lineages. Both theory and measurements indicated a higher light-reaction to CB-cycle ratio (J_{atpmax}/V_{cmax}) in C_4 than C_3. There were no evolutionary trends with photosynthetic coordination between the CB-cycle, light reactions and the C_4-cycle, suggesting strong initial selection for coordination. The coordination of CB-C_4-cycles (V_{pmax}/V_{cmax}) was optimal for CO_2 of 200 ppm, not to current conditions. Our model indicated that a higher than optimal V_{pmax}/V_{cmax} affects assimilation minimally, thus lessening recent selection to decrease V_{pmax}/V_{cmax}.

KEYWORDS

C_4 photosynthesis, electron transport, evolution, grass, optimality, J_{max}/V_{cmax}, V_{pmax}/V_{cmax}

1 | INTRODUCTION

C_4 photosynthesis evolved in response to inefficiencies of C_3 photosynthesis, which become exacerbated under certain environmental conditions: high temperature, low CO_2, drought, and highlight (Edwards et al., 2010; Ehleringer et al., 1997; Ehleringer & Monson, 1993; Zhou et al., 2018). Rubisco, the CO_2 carboxylating enzyme of the Calvin–Benson (CB) cycle, can also assimilate O_2 as the first reaction of photorespiration, a reaction that can reduce CB cycle efficiency up to 30% in C_3 species (Bauwe et al., 2010; Ehleringer et al., 1991; Raines, 2011). The C_4 pathway concentrates CO_2 around Rubisco, dramatically reducing photorespiration by segregating CO_2 uptake by phosphoenolpyruvate carboxylase (PEPc) within mesophyll cells and the assimilation of CO_2 into the CB cycle within bundle-sheath cells. However, the operation of the C_4 carbon concentrating mechanism (CCM) has additional ATP costs that are not required by C_3 plants, which photosynthesize using solely the CB cycle (Hatch, 1987).

The description above details a generic C_4 pathway, but the C_4 CCM has evolved independently more than 20 times in the grasses across different climate regimes (Ehleringer et al., 1997; Ehleringer & Monson, 1993; Zhou et al., 2018) and among lineages that had

diverged by millions of years (Christin et al., 2013; Lundgren & Christin, 2017; Sage, 2016). Therefore, it is worth asking which aspects of C_4 photosynthetic physiology differ across lineages, and what can any similarities or differences tell us of the evolutionary processes that shaped C_4 evolution. More specifically, we can examine how resources were reallocated between CO_2 uptake by PEPc, the CB cycle and light reactions and how selection optimized the function of the C_4 photosynthesis across lineages and through evolutionary time. A combined physiological and phylogenetic comparative analyses across independent evolutionary events can provide an estimate of the strength of selection for the integration of the CB cycle and the C_4 CCM during the initial evolution of C_4, further optimization after the evolution of the full C_4 CCM, and the expected degree of plasticity in C_4 operation as the climate has changed.

While it is well established that the evolution of the C_4 CCM required resource reallocation (mainly nitrogen) between the light reactions and the CB cycle, and a rebalancing of ATP and NADPH production relative to CO_2 assimilation (Ghannoum et al., 2010; Osborne & Sack, 2012; Ripley et al., 2007; Sage & Pearcy, 1987; Sharwood et al., 2016; Zhou et al., 2018), viewing these shifts through optimization models and phylogenetic sampling of C_3 and C_4 grasses will provide information on whether resource allocation differed as C_4 evolved across lineages, as well as an enhanced mechanistic explanation of resource allocation in C_4. We propose that the relative ratios between maximal Rubisco carboxylation rate (V_{cmax}), maximal electron transport (J_{max}) and maximal PEP carboxylation rate (V_{pmax}) represent the coordination within CB cycle and between CB and C_4 cycles, and offer insight into resource allocation. Although J_{max}/V_{cmax} has been empirically measured (Wullschleger, 1993) and examined with optimal modelling results in numerous C_3 species (Kromdijk & Long, 2016; Quebbeman & Ramirez, 2016; Walker et al., 2014), there have been far fewer measurements in C_4 species, and even fewer attempts to assess optimal predictions for J_{max}/V_{cmax} and the coordination of the CB cycle with the C_4 CCM, represented by V_{pmax}/V_{cmax}.

Changes, or lack thereof, in the ratios of J_{max}/V_{cmax} and V_{pmax}/V_{cmax} across phylogenies with different temporal origins of C_4 evolution, can provide an estimate of the strength of selection for the integration of the CB cycle and the C_4 CCM, as well as give insight into the evolution of C_4 from C_3. There are several extant representations suggesting that C_4 evolved from C_3 photosynthesis through a series of apparently stable intermediates between C_3 and C_2 photosynthesis (Lundgren & Christin, 2017; Mallmann et al., 2014; Sage et al., 2018; Schüssler et al., 2017; Williams et al., 2013), but there are no known examples of intermediates to suggest a likewise gradual integration of the CB cycle with the C_4 CCM (Stata et al., 2019).

Optimization modelling of C_4 photosynthesis can predict how a trait should acclimate to a given climate regime, and can, therefore, predict responses to change and/or explain observed trends. It has been proposed that C_4 may show less plasticity and acclimation in phenotypical traits in response to global climate change, due to complex anatomical and biochemical features (Sage & McKown, 2006). Recently Pignon and Long (2020) showed support for this concept in that coordination between CB and C_4 cycles was more appropriate to low CO_2 conditions of the Pleistocene. Combining optimal predictions and empirical examination of how J_{max}/V_{cmax} and V_{pmax}/V_{cmax} vary with the environment could elucidate the acclimation capability C_4 and further show if acclimation occurs in an optimal manner.

The different C_4 grass lineages evolved at different time points and different locations and, therefore, endured different evolutionary histories both before and after the evolution of C_4. Aside from the coordination of CB and C_4 CCM, this history may be apparent in extant lineages as either a result of these different evolutionary histories or extended optimization after C_4 CCM formation (Christin & Osborne, 2014; Edwards, 2019; Heyduk et al., 2019; Sage, 2016). This diversification could be represented in evolutionary trends between photosynthetic parameters such as continuous trends in maximum photosynthesis (A_{max}) through evolutionary time, and can be examined using phylogenetic comparative methods within and among C_4 lineages and as compared to closely related C_3 grass species (Edwards et al., 2007).

To examine the points detailed above, we first improved the optimal physiology model of Zhou et al. (2018), which couples photosynthesis and nitrogen stoichiometry to predict optimal ratios of J_{max}/V_{cmax} and V_{pmax}/V_{cmax}. For electron transport, we considered ATP-related electron transport (J_{atpmax}) and NADPH-related electron transport ($J_{nadphmax}$) independently as components of J_{max} (the ratios J_{atpmax}/V_{cmax} and $J_{nadphmax}/V_{cmax}$) along with V_{pmax}/V_{cmax} (Yin et al., 2016). We then performed in vivo experiments to estimate these parameters on grass lineages including C_3 (no V_{pmax}) and C_4 selected from the PACMAD clade (Grass Phylogeny Working Group II [GPWG II], 2012; Spriggs et al., 2014). By sampling multiple independent origins of C_4 within a phylogenetic context (Cavender-Bares et al., 2009; Edwards et al., 2007), we were able to use phylogenetic comparative methods to examine the divergence of traits between C_3 and C_4 and to detect whether there are continuous evolutionary trends. In sum, we used optimality modelling, physiological measurements and phylogenetic comparative methods to examine evolutionary trends, the approach to optimality, and to gain a better formal understanding of how evolution shaped the integration of electron transport, Rubisco carboxylation and PEPC carboxylation in C_4 photosynthesis (Supporting Information: Figure S1).

2 | MATERIALS AND METHODS

2.1 | Plant material

We cultivated 30 closely related species, including 9 C_3 and 21 C_4. The species belong to eight independent origins of closely related C_3 and C_4 lineages and including NAD-ME and NADP-ME subtypes of C_4 (Supporting Information: Figure S2). Seeds were sterilized before gemination, and then transferred to 6-inch (1.5 L) pots with Fafard

#52 soil (Sungro) and grown in the University of Pennsylvania greenhouse supplemented with artificial lighting so that the average light intensity was about 1500 μmol m^{-2} s^{-1}. We randomized the placement of six replicates of each species on the benches. Daytime temperature was controlled to average of 25°C, with daytime/night temperature variation of 23.9–29.4/18.3–23.8°C; the vapour-pressure deficit (VPD) varied between 0.7 and 1.3k Pa; all the plants were watered twice daily. Plants were fertilized once per week with 300 ppm Nitrogen solution (Jacks Fertilizer; JR Peters) and 0.5 tsp of 18-6-8 slow-release Nutricote Total (Arysta LifeScience America Inc.) per pot was applied when plants were first potted. To maintain optimal plant growth, a 15-5-15 cal-mg fertilizer was used every third week. The fertilizer satisfied the regular growth of species. The average nitrogen content was 4.26% for C_3 species and 3.30% for C_4 species (Supporting Information: Figure S3).

2.2 | Gas exchange and fluorescence measurements

All measurements were performed on the most recent fully expanded leaves with six replicates per species. We measured A/C_i curves using a LI-6400XT (LI-COR Inc.) for all the species by setting the reference CO_2 concentrations as 400, 200, 50, 75, 100, 125, 150, 175, 200, 225, 250, 275, 300, 325, 350, 400, 500, 600, 700, 800, 1000, 1200, 1400 ppm under saturated light intensity of 2000 μmol m^{-2} s^{-1} (Note that light intensity was set to be greater than average growth conditions to ensure the estimation of maximal electron transport rate). Data were recorded when photosynthesis rates stabilized at a given CO_2 concentration commonly within 2–4 min. The leaf temperatures were controlled at 25°C, VPD varied at 1–1.7 kPa and the flow rate of 500 μmol s^{-1} for all measurements. The cuvette was sealed with Fun-Tak instead of the standard gasket to lessen leakiness. We also measured gas exchange with fluorescence under light intensity of 150, 100, 75, 50, 20 μmol m^{-2} s^{-1}, which we used to first obtain daytime respiration rates using gas exchange and fluorescence (Yin, Sun, Struik, & Gu, 2011; Yin, Sun, Struik, Gu, Van der Putten, et al., 2011). The estimated daytime respiration was then used as an input parameter for the following estimation methods for other photosynthesis parameters. We revised the estimation method in Sharkey et al. (2007) to estimate in vivo V_{cmax} and J_{max} for C_3 species. The estimation method of Sharkey et al. (2007) was revised to allow the changepoint between different limitation states to be freely determined (to avoid bias) between 5 and 60 Pa (Supporting Information: I). We used the estimation method in Zhou et al. (2019) for V_{cmax} and J_{max} (here equal to J_{atpmax}, because no additional NADPH is consumed in the C_4 cycle, ATP-related electron transport should be the limiting factor and electron transport should not be limited by NADPH production (Yin & Struik, 2012; Yin, Sun, Struik, & Gu, 2011; Yin, Sun, Struik, Gu, Van der Putten, et al., 2011) and V_{pmax} with one slight methodological change for C_4. Since it is thought that the region of CO_2-limited A/C_i is very narrow in C_4, we assigned the C_i regions limited by carbonic anhydrase, V_{pmax} and V_{cmax} with very low criteria of 5 Pa or below. We let the data points with C_i ranging from 5 to 60 Pa CO_2 to be freely determined by which of the four potential limitation states to minimize the estimation error, which follows Yin, Sun, Struik, Gu, Van der Putten, et al. (2011). Using this method, we avoided the potential bias of including optimal perspectives to the estimation method, which could occur when directly assigning the cross points colimited by V_{cmax}, V_{pmax} and J_{atpmax}.

Furthermore, for comparison to the measured J_{atpmax}/V_{cmax} and V_{pmax}/V_{cmax} value, we collected in vitro measured values for V_{cmax} and V_{pmax} from published research, which includes 11 studies with 87 averaged results reported under current and varying environmental conditions (Supporting Information: II). Since it is impossible to obtain in vitro J_{atpmax}, the estimation of J_{atpmax} from A/C_i curves were used. We also obtained the corresponding A/C_i curves from these studies, if they were reported, to obtain the J_{atpmax}. The combination of in vivo and in vitro measurements yield a good representation of current J_{atpmax}/V_{cmax} and V_{pmax}/V_{cmax} states in the C_4 plants.

2.3 | Chlorophyll measurements and leaf nitrogen

Chlorophyll contents were measured using the spectrophotometer method (Porra et al., 1989). We cut the fresh leaves of species into pieces of 0.5 mm long, took a photo of the fragments to measure the total leaf area (ImageJ, version 1.48) and submerged the fragments into DMF. After all the Chlorophyll was extracted and the leaves turned white, the supernatant was used to measure the absorption under 663.8 nm and 646 nm. Total Chlorophyll concentrations were calculated using the equation of Porra et al. (1989). We measured leaf nitrogen content for each sample using the CHNOS analyser (ECS4010; Costech Analytical Technologies Inc.).

2.4 | Phylogenetic comparative analysis

We extracted the dated phylogenetic tree from (i) Spriggs et al. (2014) and a non-dated phylogenetic tree from (ii) GPWG II (2012) for our measured species (Supporting Information: Figure S2). The original trees had branch classifications as C_4 or C_3. To carry over the aspect of evolutionary time, we used R package 'phytools' pruned the tips of nontarget species (species not in our collection), maintained branch lengths of our target species, and kept the branch with the original information of C_3 or C_4 (Supporting Information: Figure S2). This resulted in extracted phylogenetic trees containing only our target species. We performed the analyses for both trees to ensure that the analyses were not biased by (A) differences in the rate of evolution across lineages by using the non-dated tree (which are 'hidden' in the dated tree) nor (B) differences in age by using the dated tree (which cannot be seen in the non-dated tree). We used both trees for our analyses as more rigorous support for our results and conclusions. We fitted each of the photosynthetic parameters (A_{max}, V_{cmax}, J_{atpmax}, J_{atpmax}/V_{cmax}, Total Chl, Nitrogen, V_{pmax} and

V_{pmax}/V_{cmax}) to 10 different evolutionary models falling into Brownian Motion models (BM, traits evolve randomly in direction and distance from root states) and Ornstein–Uhlenbeck models (OU, traits evolve under stabilized selection towards root states) using the R package of 'mvMORPH' (Supporting Information: Table S1). Because different traits may follow different evolutionary processes, both evolutionary models were used to test whether there were significant differences between C_3 and C_4 or among C_4 subtypes (NADP-ME and NAD-ME) and the best-fitted models were chosen. The small-sample-size corrected version of the Akaike information criterion (AICc, the lower AICc, the better fit) and Akaike weights (AICw, the higher AICw, the better fit) were used as criteria to figure out the best-fitted model. We used the likelihood-ratio test (LRT) method to test whether one model variant performs significantly better than others and to determine whether there are significant differences between C_3 and C_4. We also extract the evolutionary ages/branch lengths for each C_4 species from both phylogenies. For each C_3/C_4 pair, the branch lengths (or ages) were measured from the most recent common ancestor of each pair to the present. We regressed the above photosynthetic traits with evolutionary ages or evolutionary branch length to detect potential evolutionary trends.

2.5 | Physiological modelling

Based on the C_3 and C_4 models constructed in Zhou et al. (2018), which incorporate the soil–plant–air water continuum into traditional C_3 and C_4 photosynthesis models (von Caemmerer, 2000; Farquhar et al., 1980), we added stochiometric correlations between photosynthesis parameters and nitrogen to consider the optimal nitrogen partition among photosynthetic systems. We also incorporated updated stoichiometric coefficients for the RuBP regeneration (electron transport) and independently considered the maximum rate of electron transport related to ATP production and the maximum rate of electron transport related to NADPH production. Different from Zhou et al. (2018), which assumed parameters similarity between C_3 and C_4 species, C_3- and C_4-specific physiological and biochemical parameters were collected from the literature used to populate the model in this study. Where relevant, we used updated values for the input parameters using the estimation methods mentioned above. The detailed model description, parameterization and modelling codes can be found in Supporting Information: III and IV. Using such a framework, we can model the optimal J_{max}/V_{cmax} and V_{pmax}/V_{cmax} simultaneously considering the following nitrogen stoichiometry:

The total nitrogen is the sum of different components (Evans, 1989):

$$N_{org} = N_P + N_E + N_R + N_S + N_O, \tag{1}$$

in which N_P represents the nitrogen in pigment proteins, N_E represents the nitrogen for the electron transport system, N_R represents the nitrogen of Rubisco, N_S represents nitrogen in soluble proteins except for Rubisco and N_O represents additional organic leaf nitrogen not invested in photosynthetic functions.

To model the optimal J_{max}/V_{cmax} and V_{pmax}/V_{cmax}, we need to consider the nitrogen stoichiometry among J_{max}, V_{cmax} and V_{pmax}. We used empirical relationships found in previous studies (Evans & Poorter, 2001; Niinemets & Tenhunen, 1997; Quebbeman & Ramirez, 2016).

$$N_P + N_E = 0.0331\chi + 0.079J_{max}, \tag{2}$$

$$N_S = vJ_{max}, \tag{3}$$

$$N_R = \frac{V_{cmax}}{6.25 \times V_{cr} \times \xi}, \tag{4}$$

$$N_{PEP} = \frac{V_{pmax}}{6.72 \times V_{pr} \times \xi}, \tag{5}$$

χ is the concentration of chlorophyll per unit area (μmol Chl m^{-2}), 0.079 is in mmol N s (μmol) ^{1} representing the electron transport protein nitrogen required per μmol electron transport, and 0.0331 is in mmol N $(\mu mol\ Chl)^{-1}$ representing pigment protein correlated with per μmol chlorophyll, $v \approx 0.3$ mmol Ns $(\mu\ mol)^{-1}$ representing nitrogen of soluble protein related to per μmol electron transport. V_{cr} is the specific activity of Rubisco (the maximum rate of RuBP carboxylation per unit Rubisco; ≈20.5 μmol CO_2 (g Rubisco)$^{-1}$ s^{-1} for C_3 and 1.46 times this value for C_4) and 6.25 is grams RuBisCO per gram nitrogen in RuBisCO. V_{pr} is the specific activity of PEPc, that is, the maximum rate of RuBP carboxylation per unit PEPc [≈181.7 μmol CO_2 (g PEPC)$^{-1}$ s^{-1}], 6.72 is grams PEPc per gram nitrogen in PEPC (calculated from the amino acids composition of Fujita et al., 1984), and ξ is the mass in grams of one millimole of nitrogen equal to 0.014 g N $(mmol\ N)^{-1}$.

Further, we simplify Equation (2) by assuming there is a coordination of resource allocation between chlorophyll and electron transport for saturated light intensity, which determines the J_{max}. We make this assumption for the light-saturated condition and use the empirical equation of Croft et al. (2017) to Equation (2)

$$\chi = \frac{\frac{1000\ J_{max}}{2.49}}{\eta}, \tag{6}$$

where η is the average molar mass for chlorophyll (900 g/mol). Thus,

$$N_{org} - N_O = 0.079J_{max} + 0.0331\chi + v\ J_{max} + \frac{V_{cmax}}{6.25 \times V_{cr} \times \xi} + \frac{V_{pmax}}{6.72 \times V_{pr} \times \xi}, \tag{7}$$

For the C_3 pathway, all the nitrogen modelling processes are similar to C_4 and a same value of $N_{org} - N_O$ is used, except that a simplified version of Equation (7) is used as below (Quebbeman & Ramirez, 2016):

$$N_{org} - N_O = 0.079J_{max} + 0.0331\chi + vJ_{max} + \frac{V_{cmax}}{6.25 \times V_{cr} \times \xi}, \tag{8}$$

Because we did not find reliable coefficients for Equations (2), (3) and (6) in the literature for C_4, we assumed them the same for C_3 and

C_4. We also evaluated the potential effects of this assumption using sensitivity analysis (see Section 4). In the optimal modelling processes, we set $N_{org} - N_O$ as constant of 80 mmol N m^{-2} (which yields a V_{cmax} = 39 μmol m^{-2} s^{-1}, J_{atpmax} = 195 μmol m^{-2} s^{-1} and V_{pmax} = 78 μmol m^{-2} s^{-1}, if assuming J_{atpmax}/V_{cmax} = 5 and V_{pmax}/V_{cmax} = 2 similar to previous papers [Collatz et al., 1992; Osborne & Sack, 2012]). Using these models, we modelled the assimilation rates with different J_{atpmax}/V_{cmax} from 1 to 8 of 0.01 interval and different V_{pmax}/V_{cmax} from 0.5 to 5 of 0.01 to find the globally optimal assimilation rate with respect to both J_{atpmax}/V_{cmax} and V_{pmax}/V_{cmax}. The corresponding J_{atpmax}/V_{cmax} and V_{pmax}/V_{cmax} under the highest assimilation rates represent the optimal ratios. Then, we also modelled the locally optimal J_{max}/V_{cmax} and V_{pmax}/V_{cmax} when constraining the corresponding V_{pmax}/V_{cmax} and J_{max}/V_{cmax} with the average measured values, respectively.

For J_{max}, we consider both maximal electron transport for ATP formation (J_{atpmax}) and for NADPH formation ($J_{nadphmax}$). Using the model described above, we were able to model the optimal J_{atpmax}/V_{cmax} and $J_{nadphmax}/V_{cmax}$ individually through updating the equations related to electron transport in the original models and stoichiometry (Equations 9 and 10).

$$A_{j,atp} = \frac{(1-x)J_{atpmax}(C_{bs} - \gamma \times O_{bs})}{x_1 C_{bs} + x_2 \gamma \times O_{bs}} - R_d, \quad (9)$$

$$A_{j,nadph} = \frac{J_{nadphmax}(C_{bs} - \gamma \times O_{bs})}{x_1 C_{bs} + x_2 \gamma \times O_{bs}} - R_d, \quad (10)$$

The stoichiometry for C_4 subtypes of NADP-ME and NAD-ME were considered similar (Takabayashi et al., 2005; Y. Wang et al., 2014; Yin & Struik, 2012). Electron transport relationships are x_1 = 4 and x_2 = 28/3 for Equation (9) and x_1 = 4 and x_2 = 8 for Equation (10). Here x denotes the electron transport allocated to the C_4 cycle, which was assumed to be 0.4.

First, we modelled optimal J_{atpmax}/V_{cmax}, $J_{nadphmax}/V_{cmax}$ and V_{pmax}/V_{cmax} under saturated light intensity similar to the experimental measurements and atmospheric CO_2 of 400 ppm and 25°C with two water-availability schemes to allow for variation in water supply: VPD = 1.25 kPa, ψ_S = −1 MPa and VPD = 0.625 kPa, ψ_S = −0.5 MPa (we considered these two different water conditions to represent the potential variability in our growth condition). We then modelled the optimal J_{atpmax}/V_{cmax}, $J_{nadphmax}/V_{cmax}$ and V_{pmax}/V_{cmax} under a series of environmental gradients: atmospheric CO_2 of 200, 300, 400, 500 and 600 ppm; VPD and ψ_S of (0 MPa, −0.15 kPa) (0.625, −0.5), (1.25, −1), (1.875, −1.5) and (2.5, −2); the temperature of 15, 20, 25, 30 and 35°C. We did not model different light intensities because the light response for C_4 requires multiple parameters for which there are not yet established values. To analyse the effects of different nitrogen content, we performed sensitivity analysis for the nitrogen (from 100% to 50% with 10% interval of the regular nitrogen considered above) for optimal J_{atpmax}/V_{cmax}, $J_{nadphmax}/V_{cmax}$ and V_{pmax}/V_{cmax}. Since there is potential uncertainty for stochiometric relationships, other physiological parameters and enzyme kinetics, we performed sensitivity analysis for mesophyll conductance, bundle sheath conductance, Michalis–Menten constants of Rubisco carboxylation (K_c), Michalis–Menten constants of PEP carboxylation (K_p), the stoichiometry of Rubisco, $1/(6.25 \times V_{cr} \times \xi)$ term in Equation (4), the stoichiometry of the PEPC, $1/(6.72 \times V_{pr} \times \xi)$ term in Equation (5) and the stoichiometry of electron transport $(0.079 + 0.031 \times \frac{1000}{2.49}/\eta + v)$ term in Equation (7), from 50% to 400%.

Using the model, we also simulated the effect of decreasing V_{cmax} on the assimilation rate of both the C_3 and C_4 pathways. In this modelling process, we hold J_{atpmax}, V_{pmax} and other photosynthetic parameters constant as the initial modelling condition as above, but varying the V_{cmax} to 100%, 90%, 80%, 70%, 60% and 50% of the original values of C_3.

3 | RESULTS

3.1 | C_4 had higher J_{atpmax}/V_{cmax} and higher Chl a/b than C_3

Phylogenetic comparative analysis showed the J_{atpmax}/V_{cmax} followed the OU model, a stable evolutionary process and C_4 had a higher J_{atpmax}/V_{cmax} than C_3 species did (Table 1; Figure 1a). We looked further into how such a higher J_{atpmax}/V_{cmax} in C_4 was reached by comparing individual empirical parameters. C_4 species had equivalent stable states of J_{atpmax} in the evolutionary model, but significantly lower stable states of V_{cmax} and nitrogen content than closely related C_3 species (Table 1). Also, C_4 had a significantly higher Chl a/b ratio than that in their closely related C_3, but a lower nitrogen content (Table 1). For most of the traits, the evolutionary model did not detect significant differences between NADP-ME and NAD-ME subtypes, but NAD-ME had a higher V_{pmax} than NADP-ME (Supporting Information: Tables S2–S9). The empirical results for our phylogenetically controlled comparisons were shown in Supporting Information: Figure S3.

3.2 | *A_{max}, J_{atpmax}, total chlorophyll, V_{cmax} and V_{pmax} were positively correlated with evolutionary age*

Plotting the photosynthetic parameters with evolutionary ages (ranging from 33 to 10 MYA), extracted from the above phylogenies for the multiple lineages, allowed us to look for further evolutionary trends in C_4 and their closely related C_3 species. Regressions of evolutionary age versus photosynthetic traits provided signals for long-term directional trends in photosynthetic machinery following the establishment of C_4 photosynthesis (Figure 2, Supporting Information: Figure S4). A_{max}, J_{atpmax}, total chlorophyll, V_{cmax} and V_{pmax} showed significant positive correlations with evolutionary age in C_4, but not C_3, while nitrogen, J_{atpmax}/V_{cmax} and V_{pmax}/V_{cmax} did not show significant correlation with evolutionary age.

TABLE 1 Phylogenetic comparative results of the best-fitted evolutionary models and their parameters for photosynthesis parameters (detailed description of the models are in Supporting Information: Table S1; results summarizing Supporting Information: Table S2–S9)

Property	Model	Model type	AICw	Root	
				C_3	C_4
J_{atpmax}/V_{cmax}	Model 6[a]	OU	0.706	1.56	5.25
V_{cmax}	Model 6[a]	OU	0.695	58.30	21.30
J_{atpmax}	Model 1	BM	0.293	107.59	
Total Chl	SubtypeModel 3	BM	0.448	0.40	0.36/0.35
Chl a/b	Model 6[a]	OU	0.564	3.26	4.19
V_{pmax}	SubtypeModel 4[a]	OU	0.465		52.09/60.66
V_{pmax}/V_{cmax}	Model 1	BM	0.456		2.11
Nitrogen	Model 6[a]	OU	0.622	3.72	2.59

Note: BM represents the Brownian Motion model (traits evolve randomly in direction and distance from root states, Model 1–4 and SubtypeModel 1–3) and OU represents the Ornstein-Uhlenbeck Model (traits evolve under stabilized selection towards root states, Model 5–6 and SubtypeModel 4). Models were used to test whether C3, C4 and C4 subtypes (NADP-ME and NAD-ME) have different evolutionary states. Root represents stable-state estimation from the evolutionary models. If the root values for C3 and C4 were different, it meant there were significant different values for C3 and C4 species (the evolutionary model with two different values of the root fit significantly better than the evolutionary model with the similar root). If the root values for C4 have a '/', it means the C4 subtypes (NADP-ME/NAD-ME) are different.

[a]Whether the model fits significantly better than the other models using the likelihood-ratio test. Replication number = 6.

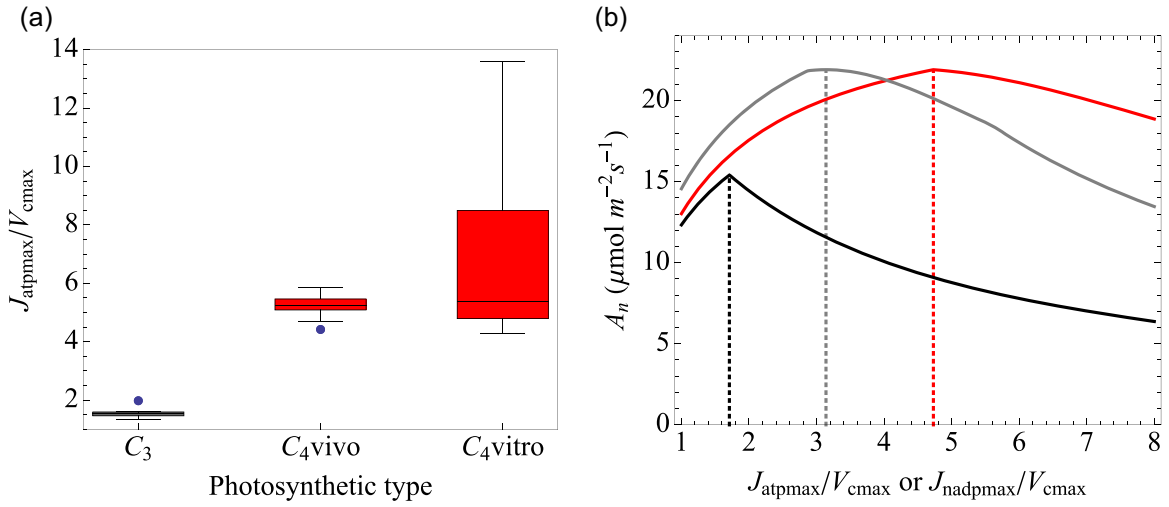

FIGURE 1 Empirical measurements (a) and optimal modelling results (b) of J_{atpmax}/V_{cmax} for C_3 and C_4 and $J_{nadpmax}/V_{cmax}$ for C_4 under ψ_S = −1 MPa, VPD = 1.25 kPa, temperature of 25°C and saturated light intensity, the cultivating environmental condition. In (b), the black line represents J_{atpmax}/V_{cmax} for C_3, solid red line represents J_{atpmax}/V_{cmax} for C_4 modelling results with controlling V_{pmax}/V_{cmax} at the in vivo measurement level, grey line represents $J_{nadpmax}/V_{cmax}$ for C_4 modelling results with controlling V_{pmax}/V_{cmax} at the in vivo measurement level.

3.3 | Measured J_{atpmax}/V_{cmax} follow modelled global optima in C_4, but V_{pmax}/V_{cmax} did not

Although J_{atpmax}, V_{cmax} and V_{pmax} showed variations across measured in vivo measurements, in vivo J_{atpmax}/V_{cmax} were consistent with the optimal predictions under current atmospheric CO_2 conditions of 400 ppm (Figures 1 and 3). In contrast, measurement-derived V_{pmax}/V_{cmax} fell into the optimal range under atmospheric CO_2 of 200 ppm (Figures 3 and 4). The global optima modelling results indicated maximal photosynthesis at the J_{atpmax}/V_{cmax} of 4.5–5.5, while the optimal range for V_{pmax}/V_{cmax} for C_4 1.4–2.0 at CO_2 of 200 ppm, but decreasing to 0.8–1.4 when CO_2 reached 400 and 600 ppm (Figure 3, Supporting Information: Figure S5). The averaged in vitro (data gathered from the literature) and in vivo (this study) J_{atpmax}/V_{cmax} were consistent with the global optimal predictions under CO_2 of 400 ppm (Figures 1a and 3, Supporting Information: Figures S5a,

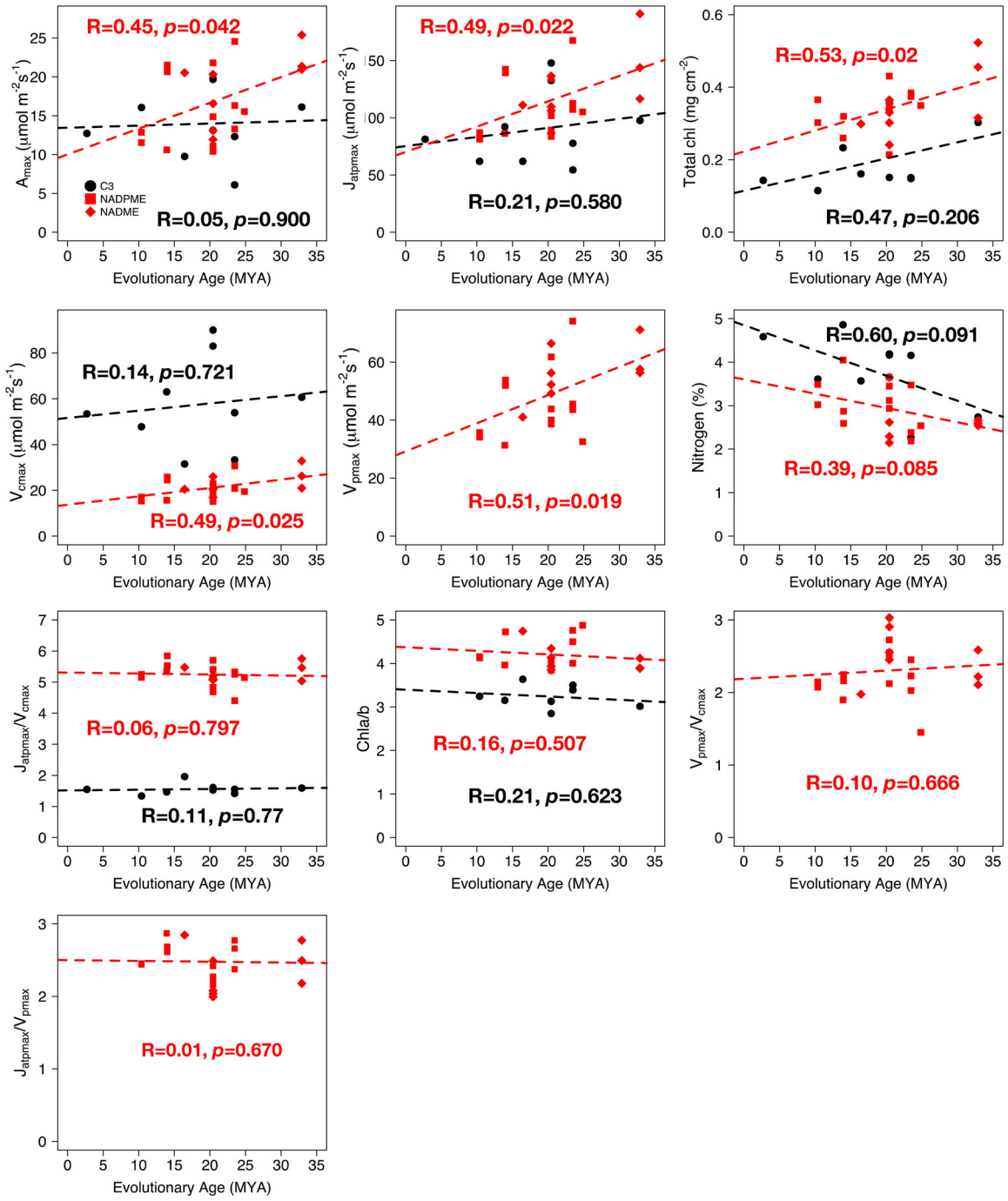

FIGURE 2 The regression for maximal assimilation rate (A_{max}), J_{atpmax}, total chlorophyll (Total chl), V_{cmax}, V_{pmax}, nitrogen concentration, J_{atpmax}/V_{cmax}, V_{pmax}/V_{cmax}, J_{atpmax}/V_{pmax} and chla/b ratio versus the evolutionary age for the nine origins to show the evolutionary trend within C_4 (red, regression for all NADPME and NADME species, because we did not found significant differences between these two subtypes) and within their closely related C_3 species (black) using the dated phylogenetic tree of Spriggs et al. (2014). Black dot: C_3 species; red square: C_4 species of NADPME subtype; red diamond dot: C_4 species of NADME subtype. Replication number = 6. [Color figure can be viewed at wileyonlinelibrary.com]

S6, and II), as well as the locally optimal predictions controlling V_{pmax}/V_{cmax} at the in vivo and in vitro level (Figure 4, Supporting Information: Figure S7). The averages of in vitro and in vivo V_{pmax}/V_{cmax} were, however, outside of the optimal predictions of global optima at CO_2 of 400 ppm, while the measurement results were consistent with optimal conditions at CO_2 of 200 ppm (Figures 3 and 4, Supporting Information: Figure S5, S7, S8, and II). The 3D images and the contour plots also illustrated that when J_{atpmax}/V_{cmax} was at the optimal range where photosynthesis was greatest, the assimilation surface was quite flat and photosynthesis showed only a

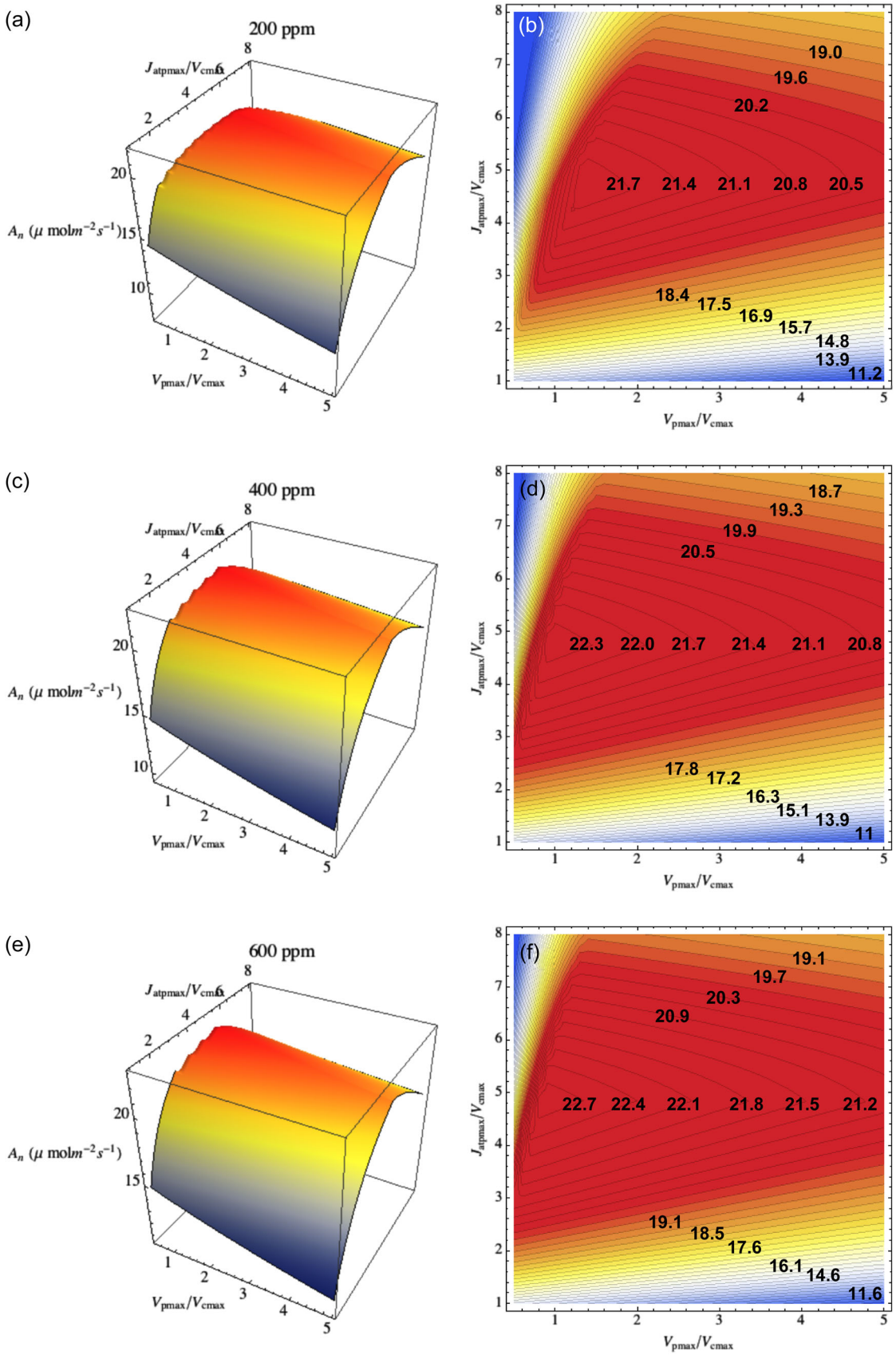

FIGURE 3 (See caption on next page)

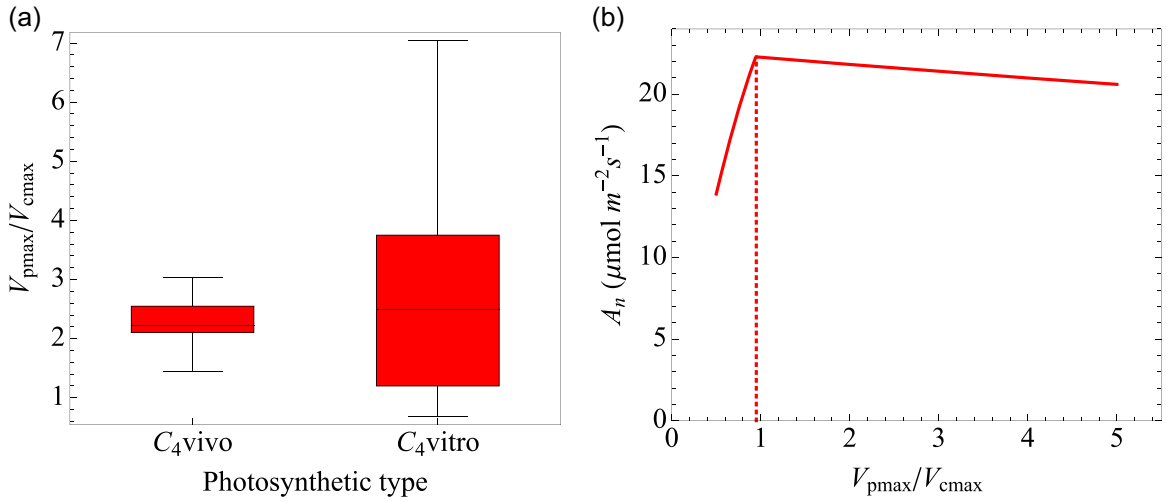

FIGURE 4 Empirical measurements (a) and optimal modelling results (b) of V_{pmax}/V_{cmax} for C_4 under ψ_S = −1 MPa, VPD = 1.25 kPa, temperature of 25°C and saturated light intensity, the cultivating environmental condition. In (b), solid red line represents C_4 modelling results with controlling J_{max}/V_{cmax} at the in vivo measurement level. VPD, vapour-pressure deficit. [Color figure can be viewed at wileyonlinelibrary.com]

mild decline as V_{pmax}/V_{cmax} moved away from optimal values. When J_{atpmax}/V_{cmax} dropped outside of the optimal ranges, however, there were sharp decreases of photosynthesis (Figure 3). Optimal results for J_{atpmax}/V_{cmax} and $J_{nadphmax}/V_{cmax}$ in C_3 species did not display large differences (Supporting Information: Figure S9). Thus, we only reported and compared J_{atpmax}/V_{cmax} in C_3 species. Optimal $J_{nadphmax}/V_{cmax}$ and J_{atpmax}/V_{cmax} were quite different for C_4. $J_{nadphmax}/V_{cmax}$ at 400 ppm was higher in C_4 (3.14) than that in C_3 (1.65), but $J_{nadphmax}/V_{cmax}$ was lower than J_{atpmax}/V_{cmax} in C_4 (Figure 1b, Supporting Information: Figure S6b). In vitro measurements indicated large variation in J_{atpmax}/V_{cmax} and V_{pmax}/V_{cmax} at the species level, which might result from true species-specific differences or from varied growth conditions across the published experiments. Such variation could lessen the comparability with our modelling results, but our in vivo results did fall into the range of in vitro results (Figures 1a and 4a). Therefore, the in vitro results could be used as at least a basic reference to indicate the potential variations of these traits in extant species.

3.4 | Decreasing V_{cmax} had little effects on the assimilation rates of C_4

As we found C_4 had a decreased V_{cmax} mentioned above, we examined the potential effects of the decreased V_{cmax} on the assimilation rate using a modelling procedure. When performing the modelling processes, we held the J_{atpmax} and V_{pmax} constant and changed the V_{cmax} from 100% to 50% of the original C_3 parameter values. A decrease in V_{cmax} would significantly decrease the assimilation rates of C_3 species from 10°C to 35°C under different atmospheric CO_2 concentrations, while decreasing V_{cmax} had little effect on the assimilation rates of C_4 species (Figure 5).

3.5 | Sensitivity analysis for optimal J_{atpmax}/V_{cmax} and V_{pmax}/V_{cmax}

There was a large variation in total nitrogen content and the multiple photosynthetic parameters (mesophyll resistance, PEPc stoichiometry, K_p, K_c, Rubisco stoichiometry, electron transport stoichiometry and bundle sheath conductance) among species. Thus, we used sensitivity analyses to examine whether these variations affected our modelling results, and we found the optimal modelling of J_{atpmax}/V_{cmax} and V_{pmax}/V_{cmax} were robust (Supporting Information: Figure S10). Variation in nitrogen content and mesophyll resistance led to significant variation in assimilation rates, however, the optimal J_{atpmax}/V_{cmax} and V_{pmax}/V_{cmax} changed little in C_3 and C_4 photosynthesis (Supporting Information: Figure S10 and S11). We modelled a less conservative nitrogen stoichiometry compared to Figure 3

FIGURE 3 Modelling results of assimilation rate with respect to maximal electron transport to maximal Rubisco carboxylation (J_{atpmax}/V_{cmax}) and maximal PEP carboxylation to maximal Rubisco carboxylation (V_{pmax}/V_{cmax}) under atmospheric CO_2 concentration of 200 (a, b), 400 (c, d) and 600 ppm (e, f). Other environmental conditions are soil water potential (ψ_s) = −1 MPa, VPD = 1.25 kPa, temperature of 25°C and saturated light intensity, a common grassland condition. Left: 3D plot (a, c, e); right: corresponding contour plot (b, d, f). 3D, 3-diemnsional; VPD, vapour-pressure deficit. [Color figure can be viewed at wileyonlinelibrary.com]

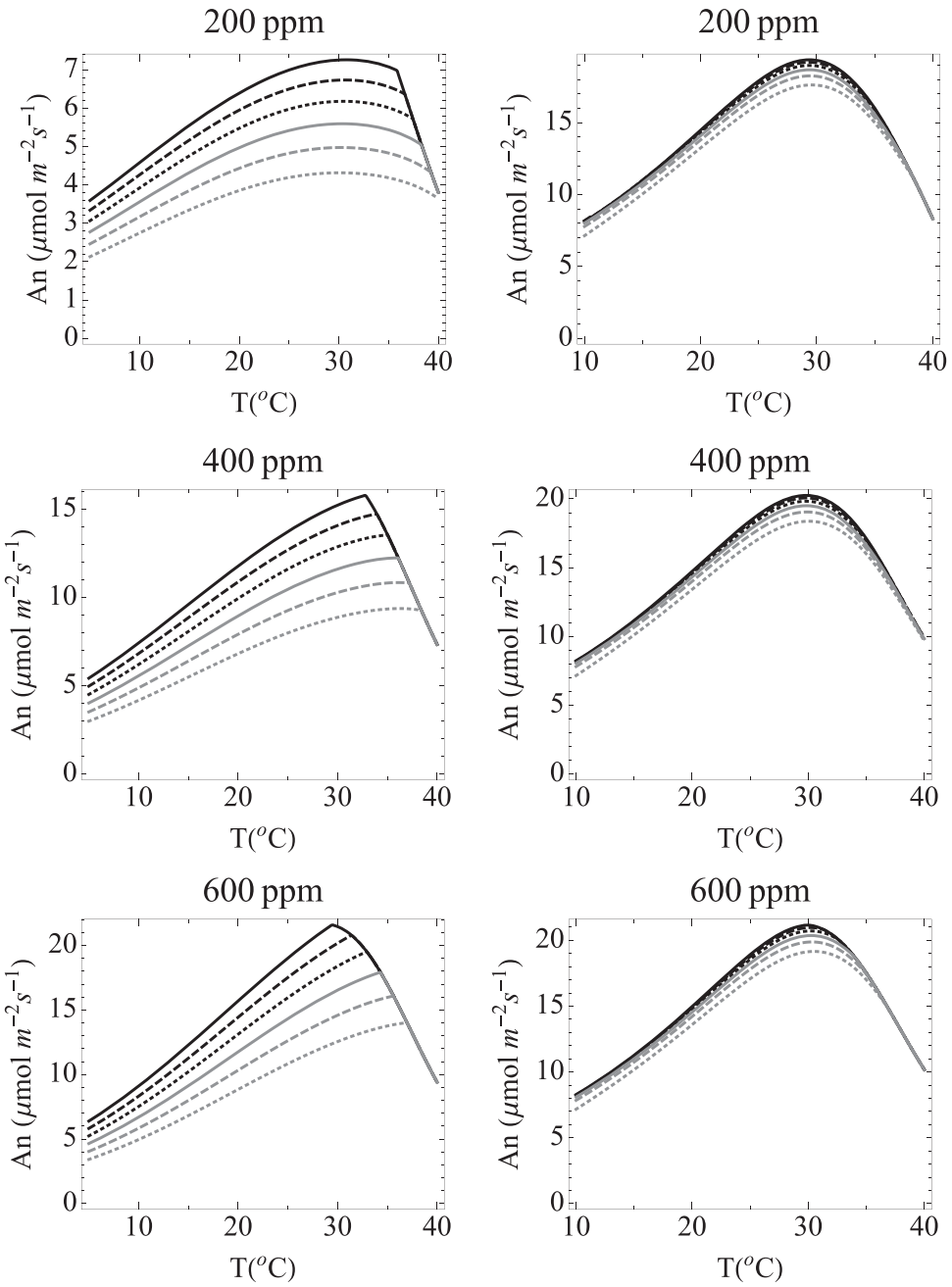

FIGURE 5 Modelling results of changing V_{cmax} on assimilation rates for C_3 (acd) and for C_4 (bdf) under different atmospheric CO_2 of 200, 400 and 600 ppm by holding other parameters as constants. Solid black line: the initial modelling condition of V_{cmax} (a typical C_3 value of 69 μmol m^{-2} s^{-1}); dashed black line: 90% of the initial V_{cmax}; dotted black line: 80% of the initial V_{cmax}; solid grey line: 70% of the initial V_{cmax}; dashed grey line: 60% of the initial V_{cmax}; dotted grey line: 50% of the initial V_{cmax}.

(33% more leaf nitrogen allocated to photosynthesis), which yielded similar and robust results compared to Figure 3 (Supporting Information: Figure S5). The optimal J_{atpmax}/V_{cmax} was relatively constant with the change of mesophyll resistance, PEPc stoichiometry and K_p and showed more variation with K_c, Rubisco stoichiometry, electron transport stoichiometry and bundle sheath conductance (Supporting Information: Figure S10 and S11). The optimal V_{pmax}/V_{cmax} was relatively robust with the change of bundle sheath conductance, K_c, Rubisco stoichiometry and electron transport stoichiometry, but showed more variation with mesophyll resistance and K_p.

3.6 | Optimal variation of J_{atpmax}/V_{cmax} and V_{pmax}/V_{cmax} with environmental conditions

To understand how the J_{atpmax}/V_{cmax} and V_{pmax}/V_{cmax} varied theoretically in response to environmental changes (Figure 6), we

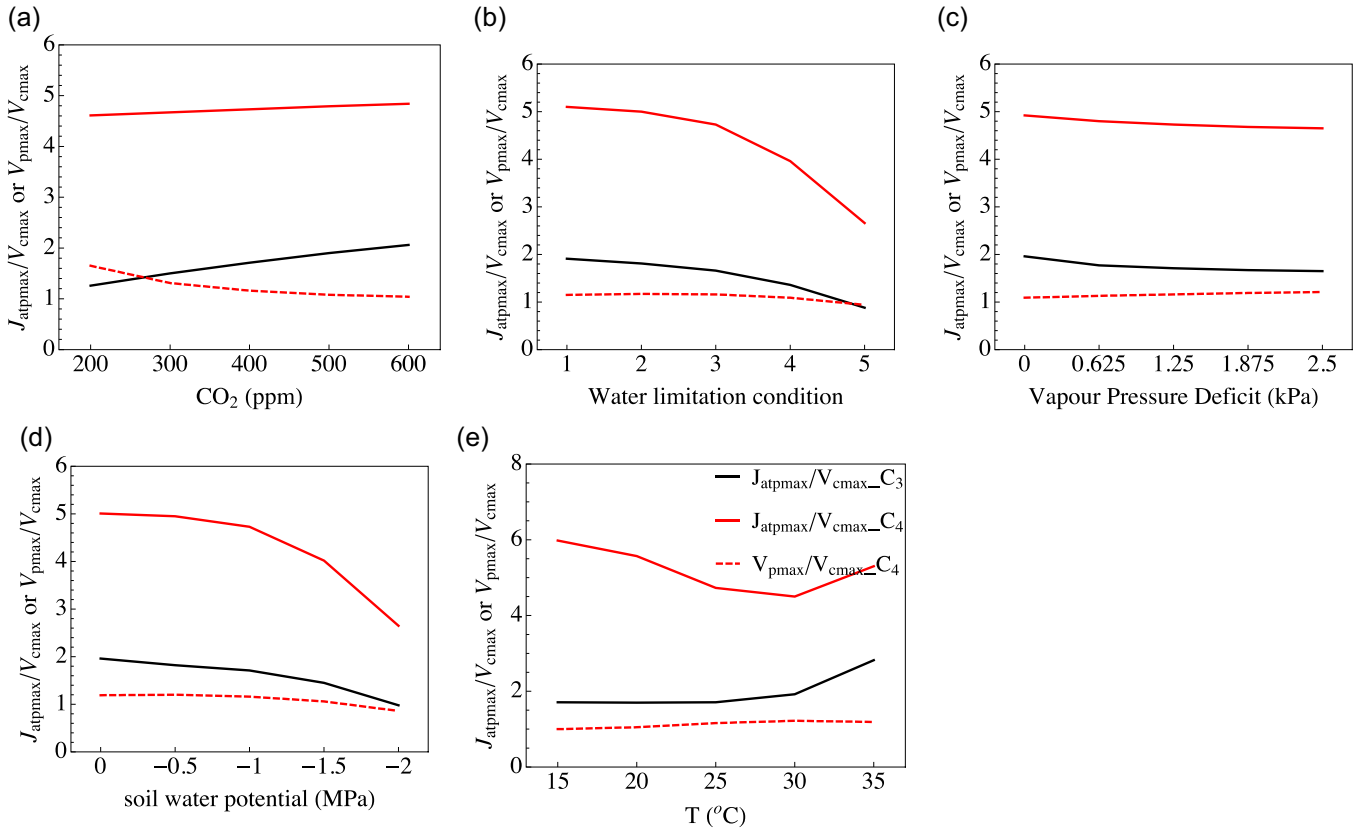

FIGURE 6 Modelling results of optimal J_{atpmax}/V_{cmax} and V_{pmax}/V_{cmax} for C_3 (black lines) and C_4 (solid and dashed red lines) under different environmental conditions. (a) different atmospheric CO_2; (b) different water limitation conditions: 1: saturated water; 2: ψ_S = −0.5 MPa, VPD = 0.625 kPa; 3: ψ_S = −1 MPa, VPD = 1.25 kPa; 4: ψ_S = −1.5 MPa, VPD = 1.875 kPa; 5: ψ_S = −2 MPa, VPD = 2.5 kPa); (c) different VPD (kPa); (d) different soil water potential (MPa); (e) different temperature. Black line: J_{atpmax}/V_{cmax} for C_3; solid red line: J_{atpmax}/V_{cmax} for C_4; dashed red line: V_{pmax}/V_{cmax} for C_4. Modelling results were obtained by controlling the other parameter at the in vivo measurement level. VPD, vapour-pressure deficit. [Color figure can be viewed at wileyonlinelibrary.com]

calculated their optimal value for varying atmospheric CO_2 concentrations, water limitations, and temperatures. The optimal J_{atpmax}/V_{cmax} was predicted to increase linearly in C_3 with a steeper slope than that in C_4 with increasing CO_2 concentration (Figure 6a). The optimal J_{atpmax}/V_{cmax} in both C_3 and C_4 decreased similarly along with increasing water limitation (Figure 6b). The J_{atpmax}/V_{cmax} decreased, then increased in C_4, but always increased in C_3, with the rise in temperature from 15°C to 35°C (Figure 6e). The changes of J_{atpmax}/V_{cmax} with water limitation and temperature were nonlinear, with the rate-of-change increasing greatly after a threshold (water limitation of ψ_S = −1, VPD = 1.25 and temperature of 30°C). The optimal V_{pmax}/V_{cmax} decreased along with the increase of the CO_2 concentration, especially when CO_2 increased from 200 to 300 ppm, but the change was little when CO_2 was above 400 ppm (Figure 6a). However, V_{pmax}/V_{cmax} was relatively constant with the varying of water limitation conditions and temperature (Figure 6b,e). Both VPD and soil water potential affected the J_{atpmax}/V_{cmax} in C_3 and C_4 species, and soil water potential showed a greater effect (Figure 6c,d, Supporting Information: Figure S12). In C_4, V_{pmax}/V_{cmax} increased slightly with the increase of VPD, and decreased with soil water potential.

4 | DISCUSSION

4.1 | Explaining the current J_{atpmax}/V_{cmax} and V_{pmax}/V_{cmax} in C_4

Our modelling efforts provide an explanation for the observed variation in J_{atpmax}/V_{cmax} and V_{pmax}/V_{cmax}, and why V_{pmax}/V_{cmax} in C_4 appears to be optimized for the lower bounds of atmospheric CO_2 of the Pleistocene (~200 ppm) (Figure 3, Supporting Information: Figure S5 and S8). Our reported values of V_{pmax}/V_{cmax} are comparable with previous studies (Kubien et al., 2003; Pengelly et al., 2010; Pignon & Long, 2020; Yin et al., 2016), and two recent papers also indicated that the coordination between CB and C_4 cycles is more appropriate for low CO_2 conditions (Pignon & Long, 2020; Sundermann et al., 2018). All extant C_4 species have gone through a low CO_2 bottleneck over the last 5 million years

(Edwards et al., 2010). This bottleneck may have resulted in a strong selection to increase V_{pmax}/V_{cmax} to maintain a high assimilation rate under the low CO_2 of glacial maxima (~200 ppm). As CO_2 has risen, first with the beginning of the Holocene interglacial, and then again with the continual burning of fossil fuels, V_{pmax}/V_{cmax} did not change along with CO_2 and consequently exceeded the optimal V_{pmax}/V_{cmax} at higher CO_2. The effects of a higher (non-optimal) V_{pmax}/V_{cmax} on assimilation rate are, however, minimal, thus the selection against a higher V_{pmax}/V_{cmax} was likely weak. The explanation directly rests on the topology of the assimilation surface: when J_{atpmax}/V_{cmax} and V_{pmax}/V_{cmax} are lower than the optimal states, the assimilation rate declines greatly; but when J_{atpmax}/V_{cmax} and V_{pmax}/V_{cmax} exceed the optimal states, the decrease of assimilation rate is minimal. The findings of non-optimal V_{pmax}/V_{cmax} indicated that such small changes in assimilation rate might open opportunities for other environmental or physiological factors, which were not modelled here, to constrain the optimization of C_4 cycle interactively. Considering interactions of multiple factors, artificial selection and manipulation to change the J_{atpmax}/V_{cmax} and V_{pmax}/V_{cmax} towards the optimal states, however, might show potential in regard to increasing total assimilation rate and productivity (Pignon & Long, 2020; Walker et al., 2018). Also, contrary to what Sage and McKown (2006) proposed, C_4 might exhibit significant acclimation capability with varying CO_2 (Pinto et al., 2014, 2016), water availability (Sharwood et al., 2014), light intensity (Pengelly et al., 2010; Sharwood et al., 2014; Sonawane, 2016) and temperature (Kubien & Sage, 2004; Pittermann & Sage, 2001; Serrano-Romero & Cousins, 2020; Sonawane, 2016) in both J_{atpmax}/V_{cmax} and V_{pmax}/V_{cmax} (Supporting Information: II, Figure 6). Finally, we note that our model applies to NADP-ME and NAD-ME subtypes in C_4, and may not be applied to PEP-CK subtypes as the ATP stoichiometry is currently unclear and likely different from NADP-ME/NAD-ME (Yin & Struik, 2018, 2021).

4.2 | Coordination within C_4 photosynthetic machinery faced strong initial selection, but the maximal assimilation rate continued to evolve

The combined physiological and phylogenetic comparative analysis shows that there were several physiological measures that changed with evolutionary age, but there were no trends with photosynthetic coordination (Figure 2, Supporting Information: Figure S4). The lack of trend with photosynthetic coordination suggests there was very strong initial selection for coordination between the CB cycle, light reactions and the C_4 CCM. This strong selection could help explain that while there are many examples of stable intermediates between C_3 and C_2 photosynthesis (Lundgren & Christin, 2017; Mallmann et al., 2014; Sage et al., 2018; Schüssler et al., 2017), there are few examples of intermediates displaying a gradual integration of the CB cycle with the C_4 CCM (Stata et al., 2019). Our analysis, therefore, supports the concept that the shift to full C_4 was more punctuated, as suggested by Stata et al. (2019), and less of a gradual shift as hypothesized by Heckmann et al. (2013). In a genome-based analysis, Bianconi et al. (2020) recently showed rapid protein changes at the initial origin of C_4 evolution within the Andropogoneae that was followed by a prolonged period of diversification of C_4 phenotypes. Their results, in concert with ours, suggest that coordination between the C_4 CCM and the CB cycle were part of this initial origin, and that this coordination was maintained as protein catalytic properties kept while other physiological measures (e.g., protein stability, turnover) changed as species spread into new ecological niches. We found distinct phylogenetic differences in several physiological measures (Figure 2), which demonstrate either selection across various habitats led to further adjustment of physiological optima as was found in the Andropogoneae (Stata et al., 2019; Williams et al., 2013) and/or phylogenetic constraints within a lineage even before the evolution of the fully integrated C_4 CCM. While speculative, we propose that changes in secondary or tertiary traits like the ratio of mesophyll cells to bundle-sheath cells, the 3D arrangement of cells and shifts in intercellular airspace could also be selected upon to increase, for example, maximum CO_2 assimilation rate through time leading to a more optimal C_4 photosynthetic machine (Alonso-Cantabrana et al., 2018; Bianconi et al., 2020; Edwards, 2019; S. Wang et al., 2017). Regardless of the mechanism, there are significant physiological differences among lineages that should be considered for future work on comparative physiology.

5 | THE MECHANISTIC AND ECOLOGICAL IMPLICATIONS OF NITROGEN REALLOCATION IN C_4

Higher J_{atpmax}/V_{cmax} and $J_{nadphmax}/V_{cmax}$ in C_4 than that in C_3 indicated a change in resource allocation, namely nitrogen, between the light reactions and the CB cycle, and as a crucial evolutionary step for elevating C_4 efficiency (Figure 1, Table 1). Because the CCM requires additional ATP and not NADPH, the optimal J_{atpmax}/V_{cmax} is higher than $J_{nadphmax}/V_{cmax}$ in C_4. However, both are higher than J_{atpmax}/V_{cmax} or $J_{nadphmax}/V_{cmax}$ in C_3 due to concentrated CO_2 in the bundle sheath. The sensitivity analyses reveal that the relative relationships between C_3 and C_4 hold, indicating that our results are robust. The modelling results indicate that a decrease of Rubisco content is favoured in C_4, because overall nitrogen requirements decrease and such a reduction has minimal effects on net assimilation rate. Significantly lower V_{cmax} in all of our C_4 and lower Rubisco in previous studies confirmed the assertion (Brown, 1978; Ku et al., 1979; Sage & Pearcy, 1987; Sharwood et al., 2016). Any surplus nitrogen not invested in Rubisco could be distributed among three broad categories: (i) Reallocated to the light reactions or ii) stored or used to construct new tissues, defense, reproduction and so on or (iii) simply not taken up from the growth environment, thus reducing total plant nitrogen requirements. Tissue et al. (1995) and Ghannoum et al. (2010) detected lower Rubisco content and higher chlorophyll and thylakoid content in C_4 species, supporting resource reallocation from RuBP carboxylation to electron transport within the leaf. Our

measurements provided evidence that the coordination of J_{atpmax}/V_{cmax} resulted from a mix of hypotheses (i) and (iii), as these hypotheses are not mutually exclusive. The significantly higher J_{atpmax} and lower V_{cmax} in C_4 than their closely related C_3 species supports a reallocation of hypothesis (i). In addition, C_4 grasses have significantly lower nitrogen content, which means C_4 had a reduced nitrogen uptake and thus, hypothesis (iii) likely occurred together with hypothesis (i). Hypothesis (ii), not exclusive to hypotheses (i) and (iii), could be supported by evidence that C_4 plants maintain larger leaf areas (Ripley et al., 2007). These hypotheses are connected to potential ecological ramifications. First, in a nitrogen-depleted habitat, C_4 could have a competitive advantage as confirmed by Ripley et al. (2007), although Sage and Pearcy (1987) found no evidence for this. In habitats where nitrogen is not limiting, the excess nitrogen could be used to construct more leaf area (Anten et al., 1995; Ripley et al., 2007; Sage & Pearcy, 1987), and greater leaf area in the early stages of growth was indeed seen by Atkinson et al. (2016). On the other hand, the lack of nitrogen reallocation from the CB cycle to the light reactions may indicate physiological constraints in fertile habitats. For example, photorespiration in C_3 plants is proposed to enhance nitrate metabolism (Bauwe et al., 2010; Bloom, 2015; Oaks, 1994; Rachmilevitch et al., 2004), therefore, the formation of CCM, which inhibits photorespiration, may reduce overall plant-available nitrogen. In addition, the increase of J_{atpmax} in C_4 could be due to an enhanced cyclic electron transport or other processes producing only ATP, not NADPH, while maintaining the linear electron transport at the same level of C_3. Elevating cyclic electron transport or other processes is, therefore, a potentially important step in engineering C_4 photosynthesis into C_3 crops.

6 | OPTIMAL J_{ATPMAX}/V_{CMAX} AND V_{PMAX}/V_{CMAX} CAN HELP TO PARAMETERIZE LAND SURFACE MODELS (LSMS)

It has recently been proposed that taking a lineage-based, or evolutionary, approach to LSMs parameterization would represent a more realistic approach to capture functional diversity (Griffith et al., 2020). In addition to the recognition of lineage-specific traits mentioned above, our work here can benefit LSMs through improved estimates of variation. In the modelling perspective, we showed that photosynthesis models were sensitive to J_{atpmax}/V_{cmax} and the lower end of V_{pmax}/V_{cmax}, thus, assigning accurate values for them is important, and our improved estimates of J_{atpmax}/V_{cmax} and V_{pmax}/V_{cmax} for C_4 plants could directly improve predictions from terrestrial biosphere models. Although J_{atpmax}, V_{cmax} and V_{pmax} are key input parameters in global-scale models (Beerling & Quick, 1995; Bonan et al., 2011; Walker et al., 2014; Zaehle et al., 2005), it is difficult and perhaps not feasible to measure all parameters for numerous sites. By utilizing the ratioed parameters described here, either J_{atpmax}/V_{cmax} and V_{pmax}/V_{cmax}, other parameters could be estimated. Using J_{atpmax}/V_{cmax} and V_{pmax}/V_{cmax} is especially crucial in C_4 because in vivo estimation of V_{cmax} and V_{pmax} is more difficult and less reliable, and in vitro measurements are not easily performed over broad taxonomic or spatial scales. We also predicted how optimal J_{atpmax}/V_{cmax} and V_{pmax}/V_{cmax} values could vary with varying environmental conditions. Such optimal behaviour could represent the plasticity or acclimation of species to environmental variations. Thus, adjusting J_{atpmax}/V_{cmax} and V_{pmax}/V_{cmax} according to these optimal predictions in LSMs could help to incorporate plant acclimation, which has long been ignored (Rogers et al., 2017; Smith & Keenan, 2020). Future greenhouse or growth chamber experiments together with our optimal modelling results would further benefit acclimation modelling.

7 | EVALUATION OF THE ASSUMPTIONS IN THE MODELLING, POTENTIAL CAVEATS AND FUTURE RESEARCH

Finally, we must highlight potential caveats and evaluate of some imperfect assumptions in the current study. We assumed C_3 and C_4 did not differ in nitrogen allocation and nitrogen stoichiometry due to the lack of reliable coefficients for equations in C_4. This is unlikely and brought some uncertainty to the results. Sensitivity analysis of Rubisco stoichiometry ($1/(6.25 \times V_{pr} \times \xi)$ in Equation 4), PEPc stoichiometry ($1/(6.72 \times V_{cr} \times \xi)$ in Equation (5) and electron transport stoichiometry ($(0.079 + 0.031 \times \frac{1000}{2.49}/\eta + v)$ in Equation 7) indicates such an assumption may have an effect on computed J_{atpmax}/V_{cmax}, but not V_{pmax}/V_{cmax} for C_4 species (Supporting Information: Figure S10). The sensitivity analysis of nitrogen mitigates the uncertainty to a degree by showing although varying nitrogen affected assimilation rates, the J_{atpmax}/V_{cmax} ratio and V_{pmax}/V_{cmax} were relatively robust (Supporting Information: Figure S10). In the current study, we used averaged values for mesophyll conductance, bundle sheath conductance, K_p and K_c collected from empirical studies in C_3 and C_4 grasses (Supporting Information: Figure S10). However, species divergences in mesophyll conductance, bundle sheath conductance, K_p and K_c also affected the J_{atpmax}/V_{cmax} ratio and V_{pmax}/V_{cmax}. For example, species with a very high mesophyll resistance or a very high K_p, could have a high V_{pmax}/V_{cmax} that is optimal to the current CO_2, but these species must be very rare considering the unrealistic mesophyll resistance and K_p. In our current study, the lack of significant differences for most traits between NADP-ME and NAD-ME species might be due to the limited species number. In the future, more detailed nitrogen stoichiometry for C_4 and a larger sampling of NADP-ME and NAD-ME species would be necessary.

8 | SUMMARY

We have provided additional mechanistic bases that the evolution of C_4 photosynthesis required the reorganization and coordination of the CB-cycle, the light reactions and the phosphoenolpyruvate carboxylase-based carbon concentrating mechanism (CCM). Strong

divergence in J_{atpmax}/V_{cmax} between C_4 and C_3 confirms that changes in resource allocation between light reactions and the CB cycle were necessary to support the enhanced ATP requirement of the C_4 CCM (Osborne & Sack, 2012; Zhou et al., 2018). Observed J_{atpmax}/V_{cmax} were within the predicted optimal zone suggesting that the resource reallocation between Rubisco carboxylation and electron transport are operating near optimality under current environmental conditions; however, the long tail exceeding the optimal J_{atpmax}/V_{cmax} in empirical measurements indicates multiple species have overallocated to electron transport, perhaps a legacy of native ecological conditions. The coordination between CB and C_4 cycles was in line with the optimal conditions under 200 ppm representing an overallocation of resources for current environmental conditions, but there is little associated cost to this departure from optimality. Rapid coordination between the CB cycle and the CCM occurred early in C_4 evolution, but it appears that C_4 photosynthesis is still under selection for further optimization. The enhanced understanding of the evolution-based photosynthetic reorganization and coordination in C_4 photosynthesis, along with our ratio-based approach to obtain photosynthetic parameters can lead to a better parameterization of terrestrial biosphere models for C_4.

ACKNOWLEDGEMENTS

We sincerely thank Dr. Matteo Detto (Princeton University) for his help in building the optimal models. H. Z. and this research is supported by the NOAA Climate and Global Change Postdoctoral Fellowship Program, administered by UCAR's Cooperative Programs for the Advancement of Earth System Science (CPAESS) under award #NA18NWS4620043B. B. H. is supported by the NSF-IOS award 1856587.

CONFLICT OF INTEREST

The authors declare no conflict of interest.

DATA AVAILABILITY STATEMENT

Data are available in the paper.

ORCID

Haoran Zhou http://orcid.org/0000-0002-5852-9535

REFERENCES

Alonso-Cantabrana, H., Cousins, A.B., Danila, F., Ryan, T., Sharwood, R.E., von Caemmerer, S. et al. (2018) Diffusion of CO_2 across the mesophyll-bundle sheath cell interface in a C_4 plant with genetically reduced PEP carboxylase activity. *Plant Physiology*, 178, 72–81.

Anten, N.P.R., Schieving, F., Medina, E., Werger, M.J.A. & Schuffelen, P. (1995) Optimal leaf area indices in C_3 and C_4 mono-and dicotyledonous species at low and high nitrogen availability. *Physiologia Plantarum*, 95, 541–550.

Atkinson, R.R.L., Mockford, E.J., Bennett, C., Christin, P.A., Spriggs, E.L., Freckleton, R.P. et al. (2016) C_4 photosynthesis boosts growth by altering physiology, allocation and size. *Nature Plants*, 2, 16038.

Bauwe, H., Hagemann, M. & Fernie, A.R. (2010) Photorespiration: players, partners and origin. *Trends in Plant Science*, 15, 330–336.

Beerling, D.J. & Quick, W.P. (1995) A new technique for estimating rates of carboxylation and electron transport in leaves of C_3 plants for use in dynamic global vegetation models. *Global Change Biology*, 1, 289–294.

Bianconi, M.E., Hackel, J., Vorontsova, M.S., Alberti, A., Arthan, W., Burke, S.V. et al. (2020) Continued adaptation of C_4 photosynthesis after an initial burst of changes in the Andropogoneae grasses. *Systematic Biology*, 69, 445–461.

Bloom, A.J. (2015) Photorespiration and nitrate assimilation: a major intersection between plant carbon and nitrogen. *Photosynthesis Research*, 123, 117–128.

Bonan, G.B., Lawrence, P.J., Oleson, K.W., Levis, S., Jung, M., Reichstein, M. et al. (2011) Improving canopy processes in the Community Land Model version 4 (CLM4) using global flux fields empirically inferred from FLUXNET data. *Journal of Geophysical Research*, 116(G2), G02014.

Brown, R.H. (1978) A difference in N use efficiency in C_3 and C_4 plants and its implications in adaptation and evolution 1. *Crop Science*, 18, 93–98.

von Caemmerer, S. (2000) Biochemical models of photosynthesis, *Techniques in plant sciences*. Colingwood, Australia: CSIRO Publishing, pp. 91–122.

Cavender-Bares, J., Kozak, K.H., Fine, P.V.A. & Kembel, S.W. (2009) The merging of community ecology and phylogenetic biology. *Ecology Letters*, 12, 693–715.

Christin, P.A. & Osborne, C.P. (2014) The evolutionary ecology of C_4 plants. *New Phytologist*, 204, 765–781.

Christin, P.A., Osborne, C.P., Chatelet, D.S., Columbus, J.T., Besnard, G., Hodkinson, T.R. et al. (2013) Anatomical enablers and the evolution of C4 photosynthesis in grasses. *Proceedings of the National Academy of Sciences*, 110, 1381–1386.

Collatz, G., Ribas-Carbo, M. & Berry, J. (1992) Coupled photosynthesis-stomatal conductance model for leaves of C_4 plants. *Functional Plant Biology*, 19(5), 519–538.

Croft, H., Chen, J.M., Luo, X., Bartlett, P., Chen, B. & Staebler, R.M. (2017) Leaf chlorophyll content as a proxy for leaf photosynthetic capacity. *Global Change Biology*, 23, 3513–3524.

Edwards, E.J. (2019) Evolutionary trajectories, accessibility and other metaphors: the case of C_4 and CAM photosynthesis. *New Phytologist*, 223, 1742–1755.

Edwards, E.J., Osborne, C.P., Strömberg, C.A.E., Smith, S.A., Bond, W.J., Christin, P.A. et al. (2010) The origins of C4Grasslands: integrating evolutionary and ecosystem science. *Science*, 328, 587–591.

Edwards, E.J., Still, C.J. & Donoghue, M.J. (2007) The relevance of phylogeny to studies of global change. *Trends in Ecology & Evolution*, 22, 243–249.

Ehleringer, J.R., Cerling, T.E. & Helliker, B.R. (1997) C_4 photosynthesis, atmospheric CO_2, and climate. *Oecologia*, 112, 285–299.

Ehleringer, J.R. & Monson, R.K. (1993) Evolutionary and ecological aspects of photosynthetic pathway variation. *Annual Review of Ecology and Systematics*, 24, 411–439.

Ehleringer, J.R., Sage, R.F., Flanagan, L.B. & Pearcy, R.W. (1991) Climate change and the evolution of C_4 photosynthesis. *Trends in Ecology & Evolution*, 6, 95–99.

Evans, J. (1989) Partitioning of nitrogen between and within leaves grown under different irradiances. *Functional Plant Biology*, 16, 533–548. Available from: https://doi.org/10.1071/PP9890533

Evans, J. & Poorter, H. (2001) Photosynthetic acclimation of plants to growth irradiance: the relative importance of specific leaf area and nitrogen partitioning in maximizing carbon gain. *Plant, Cell & Environment*, 24, 755–767.

Farquhar, G.D., Von Caemmerer, S. & Berry, J.A. (1980) A biochemical model of photosynthetic CO_2 assimilation in leaves of C3 species. *Planta*, 149, 78–90.

Fujita, N., Miwa, T., Ishijima, S., Izui, K. & Katsuki, H. (1984) The primary structure of phosphoenolpyruvate carboxylase of *Escherichia coli*. Nucleotide sequence of the ppc gene and deduced amino acid sequence. *The Journal of Biochemistry*, 95, 909–916.

Ghannoum, O., Evans, J.R. & von Caemmerer, S. (2010) Nitrogen and water use efficiency of C_4 plants. In: Raghavendra, A.S. & Sage, R.F. (Eds.) *C_4 photosynthesis and related CO_2 concentrating mechanisms*. The Netherlands, Dordrecht: Springer Science, pp. 129–146.

Grass Phylogeny Working Group II (GPWG II). (2012) New grass phylogeny resolves deep evolutionary relationships and discovers C_4 origins. *New Phytologist*, 193, 304–312.

Griffith, D.M., Osborne, C.P., Edwards, E.J., Bachle, S., Beerling, D.J., Bond, W.J. et al. (2020) Lineage-based functional types: characterising functional diversity to enhance the representation of ecological behaviour in Land Surface Models. *New Phytologist*, 228, 15–23.

Hatch, M.D. (1987) C4 photosynthesis: a unique elend of modified biochemistry, anatomy and ultrastructure. *Biochimica et Biophysica Acta (BBA)-Reviews on Bioenergetics*, 895, 81–106.

Heckmann, D., Schulze, S., Denton, A., Gowik, U., Westhoff, P., Weber, A.P.M. et al. (2013) Predicting C4 photosynthesis evolution: modular, individually adaptive steps on a Mount Fuji fitness landscape. *Cell*, 153(7), 1579–1588.

Heyduk, K., Moreno-Villena, J.J., Gilman, I.S., Christin, P.A. & Edwards, E.J. (2019) The genetics of convergent evolution: insights from plant photosynthesis. *Nature Reviews Genetics*, 20, 485–493.

Kromdijk, J. & Long, S.P. (2016) One crop breeding cycle from starvation? how engineering crop photosynthesis for rising CO_2 and temperature could be one important route to alleviation. *Proceedings of the Royal Society B: Biological Sciences*, 283, 20152578.

Ku, M.S.B., Schmitt, M.R. & Edwards, G.E. (1979) Quantitative determination of RuBP carboxylase-orygenase protein in leaves of several C_3 and C_4 plants. *Journal of Experimental Botany*, 114, 89–98.

Kubien, D.S., von Caemmerer, S., Furbank, R.T. & Sage, R.F. (2003) C_4 photosynthesis at low temperature. A study using transgenic plants with reduced amounts of Rubisco. *Plant Physiology*, 132, 1577–1585.

Kubien, D.S. & Sage, R.F. (2004) Low-temperature photosynthetic performance of a C_4 grass and a co-occurring C_3 grass native to high latitudes. *Plant, Cell & Environment*, 27, 907–916.

Lundgren, M.R. & Christin, P.A. (2017) Despite phylogenetic effects, C_3–C_4 lineages bridge the ecological gap to C_4 photosynthesis. *Journal of Experimental Botany*, 68(2), 241–254.

Mallmann, J., Heckmann, D., Bräutigam, A., Lercher, M.J., Weber, A.P., Westhoff, P. et al. (2014) The role of photorespiration during the evolution of C_4 photosynthesis in the genus *Flaveria*. *eLife*, 3, e02478.

Niinemets, Ü. & Tenhunen, J.D. (1997) A model separating leaf structural and physiological effects on carbon gain along light gradients for the shade-tolerant species *Acer saccharum*. *Plant Cell & Environment*, 20, 845–866.

Oaks, A. (1994) Efficiency of nitrogen utilization in C_3 and C_4 cereals. *Plant Physiology*, 106, 407–414.

Osborne, C.P. & Sack, L. (2012) Evolution of C_4 plants: a new hypothesis for an interaction of CO_2 and water relations mediated by plant hydraulics. *Philosophical Transactions of the Royal Society, B: Biological Sciences*, 367, 583–600.

Pengelly, J.J.L., Sirault, X.R.R., Tazoe, Y., Evans, J.R., Furbank, R.T. & von Caemmerer, S. (2010) Growth of the C_4 dicot *Flaveria bidentis*: photosynthetic acclimation to low light through shifts in leaf anatomy and biochemistry. *Journal of Experimental Botany*, 61, 4109–4122.

Pignon, C.P. & Long, S.P. (2020) Retrospective analysis of biochemical limitations to photosynthesis in 49 species: C_4 crops appear still adapted to pre-industrial atmospheric [CO_2]. *Plant, Cell & Environment*, 43, 2606–2622.

Pinto, H., Powell, J.R., Sharwood, R.E., Tissue, D.T. & Ghannoum, O. (2016) Variations in nitrogen use efficiency reflect the biochemical subtype while variations in water use efficiency reflect the evolutionary lineage of C_4 grasses at inter-glacial CO_2. *Plant, Cell & Environment*, 39, 514–CO526.

Pinto, H., Sharwood, R.E., Tissue, D.T. & Ghannoum, O. (2014) Photosynthesis of C_3, C_3–C_4, and C_4 grasses at glacial CO_2. *Journal of Experimental Botany*, 65, 3669–3681.

Pittermann, J. & Sage, R.F. (2001) The response of the high altitude C_4 grass *Muhlenbergia montana* (Nutt.) AS Hitchc. to long-and short-term chilling. *Journal of Experimental Botany*, 52, 829–838.

Porra, R.J., Thompson, W.A. & Kriedemann, P.E. (1989) Determination of accurate extinction coefficients and simultaneous equations for assaying chlorophylls a and b extracted with four different solvents: verification of the concentration of chlorophyll standards by atomic absorption spectroscopy. *Biochimica et Biophysica Acta (BBA)-Bioenergetics*, 975, 384–394.

Quebbeman, J.A. & Ramirez, J.A. (2016) Optimal allocation of leaf-level nitrogen: implications for covariation of V_{cmax} and J_{max} and photosynthetic downregulation. *Journal of Geophysical Research: Biogeosciences*, 121, 2464–2475.

Rachmilevitch, S., Cousins, A.B. & Bloom, A.J. (2004) Nitrate assimilation in plant shoots depends on photorespiration. *Proceedings of the National Academy of Sciences*, 101, 11506–11510.

Raines, C.A. (2011) Increasing photosynthetic carbon assimilation in C_3 plants to improve crop yield: current and future strategies. *Plant Physiology*, 155, 36–42.

Ripley, B.S., Abraham, T.I. & Osborne, C.P. (2007) Consequences of C_4 photosynthesis for the partitioning of growth: a test using C_3 and C_4 subspecies of *Alloteropsis semialata* under nitrogen-limitation. *Journal of Experimental Botany*, 59, 1705–1714.

Rogers, A., Medlyn, B.E., Dukes, J.S., Bonan, G., Caemmerer, S., Dietze, M.C. et al. (2017) A roadmap for improving the representation of photosynthesis in Earth system models. *New Phytologist*, 213, 22–42. Available from: https://doi.org/10.1111/nph.14283

Sage, R.F. (2016) Tracking the evolutionary rise of C_4 metabolism. *Journal of Experimental Botany*, 67, 2919–2922.

Sage, R.F. & McKown, A.D. (2006) Is C_4 photosynthesis less phenotypically plastic than C_3 photosynthesis? *Journal of Experimental Botany*, 57, 303–317.

Sage, R.F., Monson, R.K., Ehleringer, J.R., Adachi, S. & Pearcy, R.W. (2018) Some like it hot: the physiological ecology of C_4 plant evolution. *Oecologia*, 187(4), 941–966.

Sage, R.F. & Pearcy, R.W. (1987). The nitrogen use efficiency of C_3 and C_4 plants: I. Leaf nitrogen, growth, and biomass partitioning in *Chenopodium album* (L.) and *Amaranthus retroflexus* (L.). *Plant Physiology*, 84, 954–958.

Schüssler, C., Freitag, H., Koteyeva, N., Schmidt, D., Edwards, G., Voznesenskaya, E. et al. (2017) Molecular phylogeny and forms of photosynthesis in tribe Salsoleae (Chenopodiaceae). *Journal of Experimental Botany*, 68(2), 207–223.

Serrano-Romero, E.A. & Cousins, A.B. (2020) Cold acclimation of mesophyll conductance, bundle-sheath conductance and leakiness in *Miscanthus × giganteus*. *New Phytologist*, 226, 1594–1606.

Sharkey, T.D., Bernacchi, C.J., Farquhar, G.D. & Singsaas, E.L. (2007) Fitting photosynthetic carbon dioxide response curves for C_3 leaves. *Plant, Cell & Environment*, 30(9), 1035–1040.

Sharwood, R.E., Ghannoum, O. & Whitney, S.M. (2016) Prospects for improving CO_2 fixation in C_3-crops through understanding C_4-Rubisco biogenesis and catalytic diversity. *Current Opinion in Plant Biology*, 31, 135–142.

Sharwood, R.E., Sonawane, B.V. & Ghannoum, O. (2014) Photosynthetic flexibility in maize exposed to salinity and shade. *Journal of Experimental Botany*, 65, 3715–3724.

Smith, N.G. & Keenan, T.F. (2020) Mechanisms underlying leaf photosynthetic acclimation to warming and elevated CO_2 as inferred from least-cost optimality theory. *Global Change Biology*, 26, 5202–5216.

Sonawane, B.V. (2016) *Environmental regulation of CO2 concentrating mechanisms in C4 grasses with different biochemical subtypes* (Doctoral dissertation, Western Sydney University, Australia).

Spriggs, E.L., Christin, P.A. & Edwards, E.J. (2014) C_4 photosynthesis promoted species diversification during the Miocene grassland expansion. *PLoS One*, 9, e97722.

Stata, M., Sage, T.L. & Sage, R.F. (2019) Mind the gap: the evolutionary engagement of the C_4 metabolic cycle in support of net carbon assimilation. *Current Opinion in Plant Biology*, 49, 27–34. Available from: https://doi.org/10.1016/j.pbi.2019.04.008

Sundermann, E., Lercher, M. & Heckmann, D. (2018). Modeling cellular resource allocation reveals low phenotypic plasticity of C_4 plants and infers environments of C_4 photosynthesis evolution. *bioRxiv* [Preprint]. https://doi.org/10.1101/371096 [Accessed 15th April 2020].

Takabayashi, A., Kishine, M., Asada, K., Endo, T. & Sato, F. (2005) Differential use of two cyclic electron flows around photosystem I for driving CO2-concentration mechanism in C4 photosynthesis. *Proceedings of the National Academy of Sciences*, 102(46), 16898–16903.

Tissue, D.T., Griffin, K.L., Thomas, R.B. & Strain, B.R. (1995) Effects of low and elevated CO_2 on C_3 and C_4 annuals. II. Photosynthesis and leaf biochemistry. *Oecologia*, 101, 21–28.

Walker, A.P., Beckerman, A.P., Gu, L., Kattge, J., Cernusak, L.A., Domingues, T.F. et al. (2014) The relationship of leaf photosynthetic traits–V_{cmax} and J_{max}–to leaf nitrogen, leaf phosphorus, and specific leaf area: a meta-analysis and modeling study. *Ecology and Evolution*, 4, 3218–3235.

Walker, B.J., Drewry, D.T., Slattery, R.A., VanLoocke, A., Cho, Y.B. & Ort, D.R. (2018) Chlorophyll can be reduced in crop canopies with little penalty to photosynthesis. *Plant Physiology*, 176, 1215–1232.

Wang, S., Tholen, D. & Zhu, X.G. (2017) C_4 photosynthesis in C_3 rice: a theoretical analysis of biochemical and anatomical factors. *Plant, Cell & Environment*, 40, 80–94.

Wang, Y., Bräutigam, A., Weber, A.P.M. & Zhu, X.G. (2014) Three distinct biochemical subtypes of C_4 photosynthesis? A modelling analysis. *Journal of Experimental Botany*, 65(13), 3567–3578.

Williams, B.P., Johnston, I.G., Covshoff, S. & Hibberd, J.M. (2013) Phenotypic landscape inference reveals multiple evolutionary paths to C_4 photosynthesis. *eLife*, 2, e00961.

Wullschleger, S.D. (1993) Biochemical limitations to carbon assimilation in C_3 plants—A retrospective analysis of the A/C_i curves from 109 species. *Journal of Experimental Botany*, 44, 907–920.

Yin, X., Van Der Putten, P.E.L., Driever, S.M. & Struik, P.C. (2016) Temperature response of bundle-sheath conductance in maize leaves. *Journal of Experimental Botany*, 67, 2699–2714.

Yin, X. & Struik, P.C. (2012) Mathematical review of the energy transduction stoichiometries of C_4 leaf photosynthesis under limiting light. *Plant, Cell & Environment*, 35, 1299–1312.

Yin, X. & Struik, P.C. (2018) The energy budget in C4photosynthesis: insights from a cell-type-specific electron transport model. *NewPhytologist*, 218, 986–998.

Yin, X. & Struik, P.C. (2021) Exploiting differences in the energy budgetamong C4subtypes to improve crop productivity. *New Phytologist*, 229, 2400–2409.

Yin, X., Sun, Z., Struik, P.C. & Gu, J. (2011) Evaluating a new method to estimate the rate of leaf respiration in the light by analysis of combined gas exchange and chlorophyll fluorescence measurements. *Journal of Experimental Botany*, 62(10), 3489–3499.

Yin, X., Sun, Z., Struik, P.C., Van der Putten, P.E., Van Ieperen, W.I.M. & Harbinson, J. (2011) Using a biochemical C_4 photosynthesis model and combined gas exchange and chlorophyll fluorescence measurements to estimate bundle-sheath conductance of maize leaves differing in age and nitrogen content. *Plant, Cell & Environment*, 34, 2183–2199.

Zaehle, S., Sitch, S., Smith, B. & Hatterman, F. (2005) Effects of parameter uncertainties on the modeling of terrestrial biosphere dynamics. *Global Biogeochemical Cycles*, 19, GB3020.

Zhou, H., Akçay, E. & Helliker, B.R. (2019) Estimating C_4 photosynthesis parameters by fitting intensive A/C_I curves. *Photosynthesis Research*, 141, 181–194.

Zhou, H., Helliker, B.R., Huber, M., Dicks, A. & Akçay, E. (2018) C_4 photosynthesis and climate through the lens of optimality. *Proceedings of the National Academy of Sciences*, 115, 12057–12062.

SUPPORTING INFORMATION

Additional supporting information can be found online in the Supporting Information section at the end of this article.

How to cite this article: Zhou, H., Akçay, E. & Helliker, B. (2023) Optimal coordination and reorganization of photosynthetic properties in C_4 grasses. *Plant, Cell & Environment*, 46, 796–811. https://doi.org/10.1111/pce.14506